LETTER

doi:10.1038/nature16483

The *C. elegans* adult neuronal IIS/FOXO transcriptome reveals adult phenotype regulators

Rachel Kaletsky[1]*, Vanisha Lakhina[1]*, Rachel Arey[1], April Williams[1], Jessica Landis[1], Jasmine Ashraf[1] & Coleen T. Murphy[1]

Insulin/insulin-like growth factor signalling (IIS) is a critical regulator of an organism's most important biological decisions from growth, development, and metabolism to reproduction and longevity. It primarily does so through the activity of the DAF-16 transcription factor (forkhead box O (FOXO) homologue), whose global targets were identified in *Caenorhabditis elegans* using whole-worm transcriptional analyses more than a decade ago[1]. IIS and FOXO also regulate important neuronal and adult behavioural phenotypes, such as the maintenance of memory[2] and axon regeneration[3] with age, in both mammals[4] and *C. elegans*, but the neuron-specific IIS/FOXO targets that regulate these functions are still unknown. By isolating adult *C. elegans* neurons for transcriptional profiling, we identified both the wild-type and IIS/FOXO mutant adult neuronal transcriptomes for the first time. IIS/FOXO neuron-specific targets are distinct from canonical IIS/FOXO-regulated longevity and metabolism targets, and are required for extended memory in IIS *daf-2* mutants. The activity of the forkhead transcription factor FKH-9 in neurons is required for the ability of *daf-2* mutants to regenerate axons with age, and its activity in non-neuronal tissues is required for the long lifespan of *daf-2* mutants. Together, neuron-specific and canonical IIS/FOXO-regulated targets enable the coordinated extension of neuronal activities, metabolism, and longevity under low-insulin signalling conditions.

The *C. elegans* IIS pathway acts both cell autonomously and non-autonomously to control longevity, growth, dauer formation, metabolism, and reproduction[5–7] through its regulation of the nuclear localization and transcriptional activation of DAF-16 (also known as FOXO). The canonical IIS/FOXO gene set, which identified primarily intestinal and hypodermal targets (Extended Data Fig. 1a, b)[1,8,9], has been instructive in our understanding of how insulin signalling regulates a diverse range of activities, including metabolism, autophagy, stress resistance, and proteostasis. However, IIS mutants also exhibit *daf-16*-dependent neuronal phenotypes, including extended positive olfactory learning[2], increased short- and long-term associative memory[2], increased thermotaxis learning[10], improved neuronal morphology maintenance[11,12], and improved axon regeneration[3]. These phenotypes are unlikely to be regulated by the known intestinal and hypodermal IIS/FOXO targets[1,8]. Therefore, to understand how IIS *daf-2* mutant animals extend behavioural functionality, we must identify the neuronal targets of FOXO/DAF-16.

We first profiled the expression of *daf-16;daf-2* mutant worms with *daf-16* rescued in specific tissues[6] (Supplementary Table 1). Intestinal *daf-16* rescue correlates best with whole-worm profiles (Extended Data Fig. 1a, c). By contrast, neuronal *daf-16* rescue profiles are anti-correlated with the intestinal DAF-16 and whole-worm profiles (Extended Data Fig. 1a, c). Surprisingly, many genes induced by neuronal DAF-16 rescue are expressed (WormBase) or predicted to be expressed in non-neuronal tissues[13] (Extended Data Fig. 1d), and have non-neuronal functions (for example, collagens[14]; Extended Data Fig. 1b, e, Supplementary Table 2). Thus, whole-worm transcriptional analyses of neuronally rescued DAF-16 failed to reveal targets that account for *daf-16*-dependent age-related behaviours of *daf-2* mutants. Therefore, we needed to specifically examine transcription in IIS-mutant neurons.

The tough outer cuticle prevents dissociation of adult tissues[15], thus the wild-type adult neuronal transcriptome has not been described. To solve this problem, we used rapid, chilled chemomechanical disruption followed immediately by fluorescence-activated cell sorting (FACS) to isolate neurons marked with green fluorescent protein (GFP) from wild-type worms, then RNA-sequenced these isolated cells (Fig. 1a–c, Extended Data Fig. 2a–c, f, g, Supplementary Table 3). This method is gentle enough to preserve the integrity of cells and some neurites (Extended Data Fig. 2a), does not involve cell culturing before FACS, in contrast to previous methods[16], and does not affect transcription (as shown by actinomycin D treatment; Fig. 1b, Extended Data Fig. 2d, e, Supplementary Table 4). Downsampling analysis showed that sufficient sequencing depth was achieved (Extended Data Fig. 2h).

We compared gene expression in isolated wild-type neurons with whole-worm expression to identify genes that are enriched in neurons (Fig. 1a–c). Of the 1,507 'neuron-enriched' genes (false discovery rate (FDR) < 0.1; Supplementary Table 3; Fig. 1a, b), only 4% have previously described expression patterns exclusively in non-neuronal tissues, and 'Neuron' is the only significantly enriched tissue (Fig. 1c, Extended Data Fig. 2f), indicating that the method is highly selective for neuronal transcripts. Gene promoter–GFP tests of previously uncharacterized genes from our neuron-enriched list confirmed neuronal expression, with no bias for particular neuron types (Extended Data Fig. 3a). We also detected genes previously reported to be expressed only in single neurons or small subsets of neurons, including *glr-3* (in the RIA neuron), *ttx-3* (interneuron AIY/AIA) and *npr-14* (neuron AIY) (WormBase).

The wild-type neuron-enriched set includes synaptic machinery, ion channels, neurotransmitters, and signalling components (Supplementary Table 3), as well as >700 previously uncharacterized genes; these genes are predicted to have 'neuronal'-like character and function (Fig. 1d). Comparison of the wild-type embryonic and larval neuronal transcriptomes with the adult neuronal transcriptome at the same FDR revealed a shift in functional categories from developmental processes to neuronal function/behaviour in the adult neuronal transcriptome (Fig. 1e, Extended Data Fig. 3b, c, Supplementary Table 5), suggesting that previous isolation methods[16], either due to early developmental stage isolation or to re-culturing, biased expression towards developmental genes rather than neuronal/behavioural genes.

To identify adult neuronal IIS/FOXO targets, we sequenced RNA from isolated *daf-2* and *daf-16;daf-2* mutant neurons on day 1 of adulthood (Fig. 2a, Extended Data Fig. 4, Supplementary Table 6, 8). The IIS/FOXO neuron-isolated gene set is enriched for neuronal expression: 86% and 92% of the up- and downregulated genes, respectively, are expressed in wild-type neurons. While several top Class I gene

[1]Department of Molecular Biology & LSI Genomics, Princeton University, Princeton, New Jersey 08544, USA.
*These authors contributed equally to this work

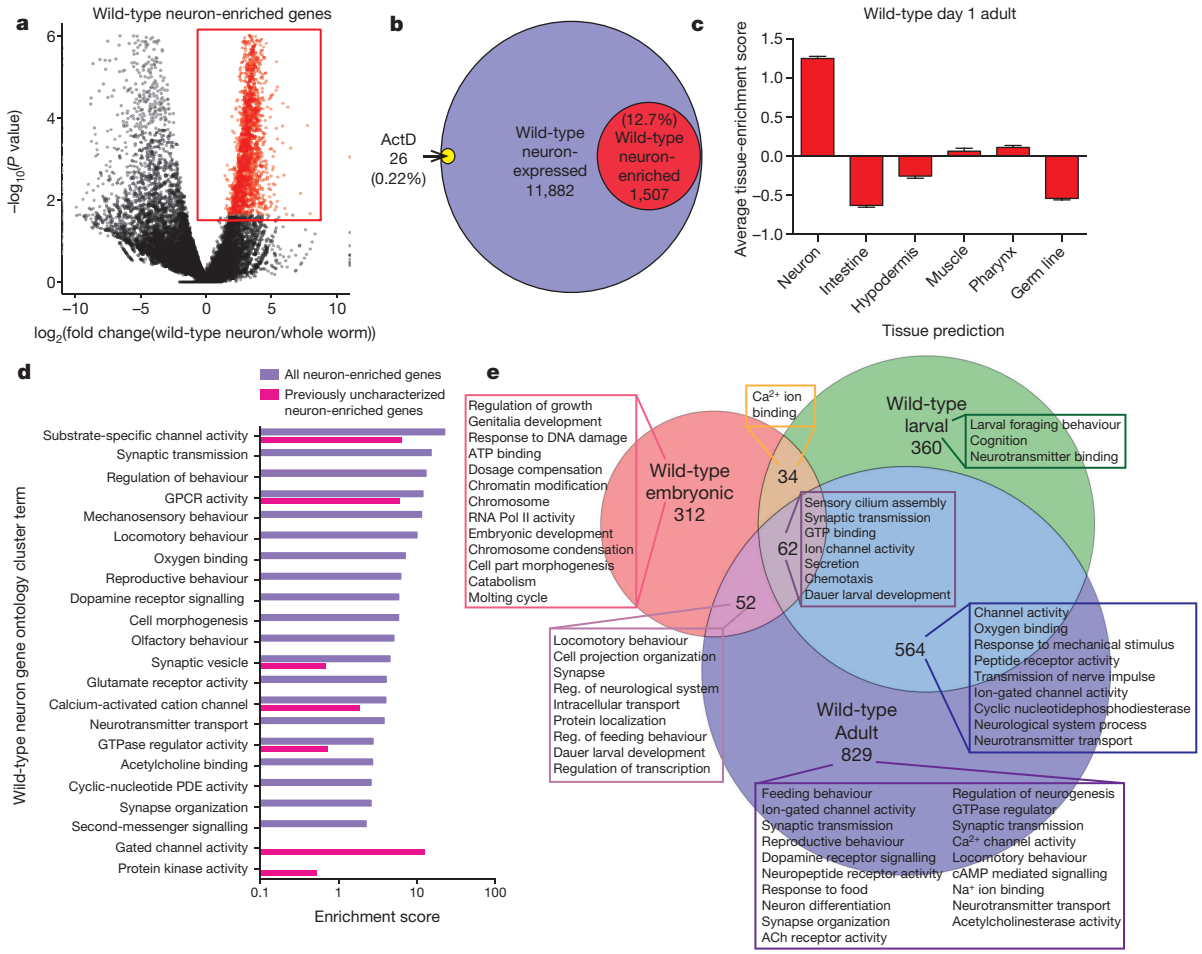

Figure 1 | Identification of neuronal IIS/FOXO targets requires neuronal isolation. a, Volcano plot of neuron-expressed relative to whole-worm-expressed genes obtained by neuron-specific RNA sequencing of adult wild-type animals. $N = 3$ biological replicates (wild-type neurons) and 2 biological replicates (whole worm). **b**, Neuron-expressed and -enriched genes are not influenced by cell isolation: treatment with the transcription inhibitor actinomycin D affected only 0.22% of all neuronal genes (Supplementary Table 4). **c**, Tissue expression prediction of wild-type adult neuron-enriched genes. Mean ± s.e.m. **d**, GO terms highlight the neuronal characteristics of both all and previously uncharacterized neuron-enriched genes. **e**, Embryonic[16], larval[16] and adult neuron-enriched genes and significant GO terms transition from developmental to neuronal and behavioural functions (Supplementary Table 5); FDR < 10% for all gene sets.

targets of DAF-16, including *hil-1*, *sip-1*, *mtl-1*, *nnt-1*, *ins-6*, and *daf-16* itself, were upregulated in both *daf-2* mutant neurons and *daf-2* mutant whole worms (Group B; Fig. 2b), most of the IIS/FOXO neuronally regulated set differs from the canonical whole-worm IIS/FOXOs set[1,8] (Fig. 2b). Specifically, in contrast to the metabolism-dominated functions of canonical whole-worm IIS/FOXO targets[1,8], the neuronal IIS set gene ontology terms reflect neuron-like functions (Extended Data Fig. 5b): serpentine receptors, G protein-coupled receptors, syntaxin, globins, kinesins, insulins, ion channels, potassium channels, seven-transmembrane receptors, the NPR-1 neuropeptide receptor, and the SER-3 octopamine receptor are upregulated in *daf-2* neurons (Supplementary Table 6). A few genes (*fat-3* and *crh-1*, a CREB homologue) are upregulated in *daf-2* neurons but downregulated in whole *daf-2* animals.

The IIS/FOXO downregulated set includes serpentine receptors, guanylate cyclases, signalling peptides and receptors (neuropeptide-like proteins, FMRF-like peptides and neuropeptides), and the vesicle trafficking G protein *rab-28* (Supplementary Table 6). Expression of the sensory neuron cilia protein IFTA-2, which co-localizes with DAF-2 and whose loss increases lifespan[17], is downregulated in *daf-2* mutants, consistent with the longevity of *daf-2* and ciliated sensory neuron mutants[18]. Similarly, *sams-1* (*S*-adenosyl methionine synthetase), which is downregulated under long-lived dietary restriction conditions[19], and *sma-5* and *dbl-1*, components of TGF-beta pathways linked with IIS[7,20], are downregulated, perhaps coordinating the longevity and reproductive output of these pathways.

Unlike canonical IIS/FOXO targets[1], neuronal IIS/FOXO gene promoters are not enriched for the DBE (DAF-16 binding element, GTAAAt/cA), but the overlapping, upregulated (Group B) targets' promoters contain twice as many DBEs (Extended Data Fig. 5a). The overlapping downregulated (Group F) targets are enriched for the PQM-1/DAE motif (CTTATCA, see refs 1, 8; Supplementary Table 7). DAF-16 may regulate neuronal activities indirectly through activation of ~60 IIS/FOXO-upregulated transcription factors (Supplementary Table 6).

We next tested the roles of top-scoring genes in *daf-2*-regulated neuronal phenotypes. Long-term and short-term associative memory are both extended in *daf-2* mutants in a *daf-16*-dependent manner[2] (Extended Data Fig. 6). The bZIP transcription factor CREB, which is required for long-term memory in many organisms, including *C. elegans*[2], is upregulated by IIS/FOXO in neurons (Supplementary Table 6), correlating with the increased long-term memory of *daf-2* mutants[2,21]. However, short-term associative memory (STAM; Fig. 2c) is CREB-independent[2], and the genes that enable STAM extension in *daf-2* mutants are unknown. While the DAF-16 non-neuronal target *sod-3* had no effect on the extended STAM of *daf-2* mutants (Fig. 2c, Extended Data Fig. 6b–d), knockdown of 8 of the 10 top-ranked, upregulated IIS/FOXO targets significantly decreased the STAM of

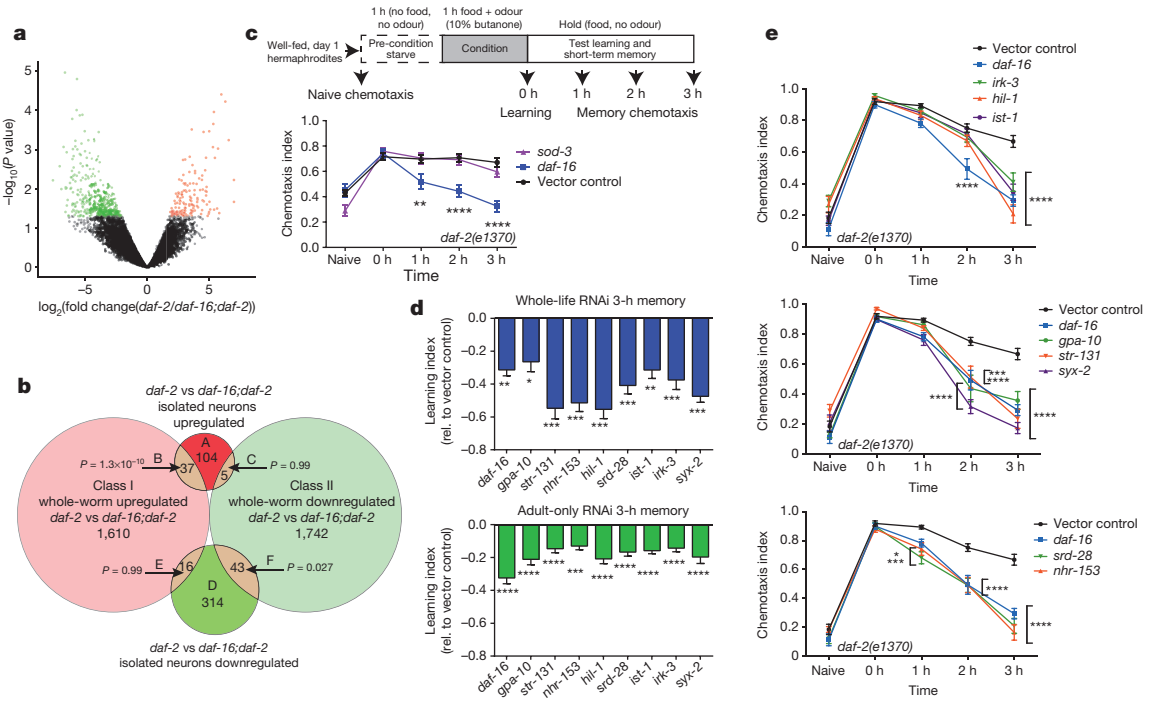

Figure 2 | RNA-seq transcriptional profile of isolated neurons reveals IIS/FOXO neuronal transcriptome. a, Volcano plot of *daf-2*-regulated, *daf-16*-dependent up- (red) and downregulated (green) neuronal genes ($P < 0.05$, $N = 4$ biological replicates per strain). **b**, Comparison of whole-worm (Class I)[8] vs neuronal-IIS/FOXO targets. *P* values: hypergeometric distributions. **c**–**e**, Short-term associative memory (STAM) assays. **c**, Schematic of STAM assay and chemotaxis profiles of *daf-2* treated with *sod-3* (**c**) or neuronal IIS/FOXO target gene RNAi (**d**, **e**). **d**, Learning indices relative to control RNAi at 3 h post-training of *daf-2* treated with adult-only (green) or whole-life (blue) neuronal IIS/FOXO target gene RNAi. Mean ± s.e.m., $^*P < 0.05$, $^{**}P < 0.01$, $^{***}P < 0.001$, $^{****}P < 0.0001$, two-way repeated measures ANOVA, Bonferroni post hoc tests. At least 3 biological replicates were performed for all STAM assays.

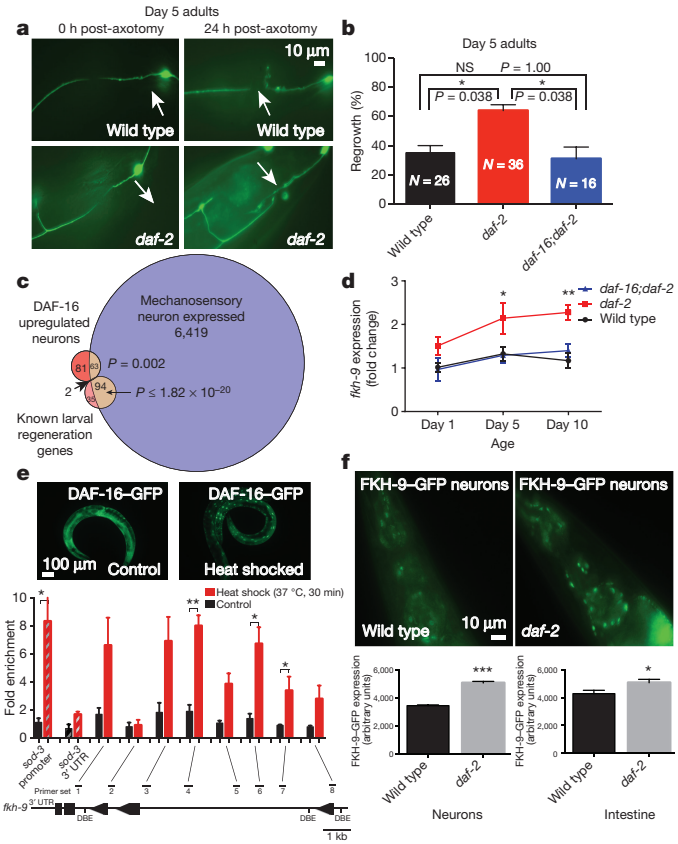

Figure 3 | FKH-9 is a direct target of DAF-16 and is expressed in mechanosensory neurons. a, **b**, *daf-16* is required for enhanced day 5 axon regeneration in *daf-2* mutants, mean ± s.e.m., $^*P < 0.05$, Fisher's exact test, $N = 26$ (wild-type), 36 (*daf-2*) and 16 (*daf-16;daf-2*), 2 biological replicates. **c**, Known larval regeneration genes are significantly enriched in the day 1 adult mechanosensory transcriptome. 63 genes are both DAF-16 targets and expressed in mechanosensory neurons (FDR < 5%; 3 biological replicates). **d**, *fkh-9* messenger RNA levels are higher in aged *daf-2* compared to wild type in a *daf-16*-dependent manner. $N = 4$ biological replicates, two-way ANOVA, Bonferroni post hoc tests. **e**, Chromatin immunoprecipitation of DAF-16–GFP worms with and without heat shock, which mobilizes DAF-16 into the nucleus. DAF-16 binds to the *sod-3* promoter but not its 3′ UTR, and to the *fkh-9* promoter at multiple locations (Extended Data Fig. 8). Fold enrichment relative to wild-type (not expressing DAF-16–GFP) is shown (mean ± s.e.m., two-tailed *t*-test, $N = 3$ biological replicates). **f**, Neuronal FKH-9–GFP (*fkh-9p::fkh-9::gfp*) expression in *daf-2* compared to wild type. $N = 25$ animals. Mean ± s.e.m., two-tailed *t*-test. **d**–**f**, $^*P < 0.05$, $^{**}P < 0.01$, $^{***}P < 0.001$.

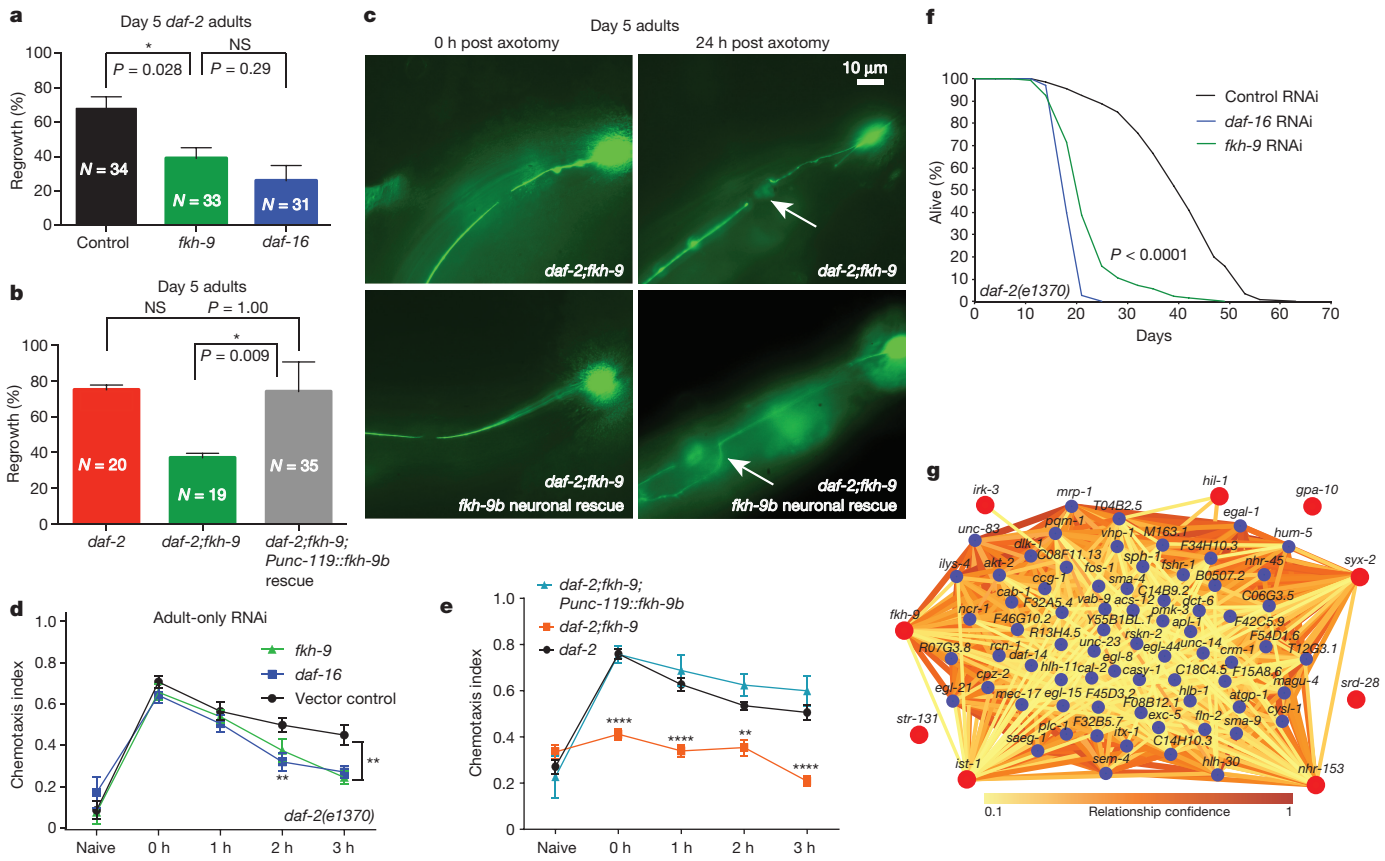

Figure 4 | FKH-9 is required for improved axon regeneration, short-term associative memory and lifespan in *daf-2* mutants. **a**, *fkh-9* knockdown reduces axon regeneration of day 5 *daf-2* mutants, as does *daf-16* knockdown. Mean ± s.e.m., $*P < 0.05$, Fisher's exact test, $N = 34$ (control), 33 (*fkh-9*) and 31 (*daf-16*), 4 biological replicates. **b**, **c**, Neuronally-expressed *fkh-9* rescues day 5 axon regeneration in *daf-2;fkh-9* mutants. Mean ± s.e.m., $*P < 0.05$, Fisher's exact test, $N = 20$ (*daf-2*), 19 (*daf-2; fkh-9*) and 35 (*daf-2; fkh-9; Punc-119::fkh-9B*, 2 biological replicates. **d**, *fkh-9* is required for enhanced memory in adult-only RNAi-treated *daf-2* mutant worms. **e**, Neuronally-expressed *fkh-9* rescues extended STAM in *daf-2;fkh-9* mutants with defective learning and memory. Mean ± s.e.m., $**P < 0.01$, $***P < 0.001$, $****P < 0.0001$, two-way repeated measures ANOVA, Bonferroni post hoc tests. **f**, Adult-specific *fkh-9* RNAi treatment reduces *daf-2* mutant lifespan. Median lifespan: control RNAi 42 days, *fkh-9* RNAi 21 days, *daf-16* RNAi 21 days. $P < 0.0001$ for control RNAi vs *daf-16* RNAi and control vs *fkh-9* RNAi, log-rank test. $N = 144$ worms per strain. **g**, Integrative Multi-species Prediction (IMP; see ref. 30) network analysis of DAF-16 neuronal target genes with STAM phenotypes (red circles).

daf-2(e1370) (Fig. 2d, e), both in whole-life and adult-only RNA interference (RNAi) tests. (Neuronal RNAi is effective in learning, STAM, and LTAM tests[21].) The variety of genes (ion channels, transcription factors, G-proteins, vesicle fusion proteins) required for *daf-2* mutants' extended STAM suggests that decreased insulin signalling affects a broad network of memory extension genes. Several of these genes are also required for learning and memory in wild type (Extended Data Fig. 6g), suggesting that *daf-2* mutants maintain neuronal function, rather than using an alternative short-term memory mechanism.

daf-2 mutants also maintain motor neuron axon regeneration ability with age in a *daf-16*-dependent manner[3], and we found this is also true for mechanosensory neurons (Fig. 3a, b, Extended Data Fig. 7a–d). To identify factors that enable axon regeneration with age, we isolated and RNA-sequenced six adult mechanosensory neurons (Fig. 3c, Supplementary Table 9); this set includes 94 known larval regeneration genes from limited candidate screens[22] ($P \leq 1.82 \times 10^{-20}$). To find *daf-2/daf-16*-dependent axon regeneration candidates, we identified mechanosensory genes that are also regulated by neuronal IIS/FOXO (Fig. 3c, Supplementary Table 9; $P < 0.002$). The forkhead transcription factor FKH-9 is a neuronal IIS/FOXO target (Supplementary Table 6) and a canonical Class I target[1], and is expressed in mechanosensory neurons (Supplementary Table 9). The *fkh-9* promoter is occupied by DAF-16, which we confirmed by chromatin immunoprecipitation followed by quantitative PCR (ChIP-qPCR; Fig. 3e, Extended Data Fig. 8a, b). FKH-9–GFP localized to nuclei, and neurons were the primary site of differential FKH-9–GFP levels in *daf-2* mutants (Fig. 3f, Extended Data Fig. 8c), all suggesting a role for FKH-9 in *daf-2/daf-16*-mediated neuronal function.

While there is no effect on the first day of adulthood (Extended Data Fig. 7e, f), loss of *fkh-9* severely impairs axon regeneration ability in aged (day 5) *daf-2* mutants (Fig. 4a), correlating with an increased difference in *fkh-9* expression levels between wild-type and *daf-2* (Fig. 3d). Pan-neuronal *fkh-9* expression rescues the ability of day 5 *daf-2;fkh-9* worms to regenerate PLM axons (Fig. 4b, c). *fkh-9* levels are critical for neuron morphology, as *fkh-9* neuronal overexpression causes axonal defects (Extended Data Fig. 7g).

Adult-specific and whole-life reduction of *fkh-9* also severely impaired extended STAM of *daf-2* mutants (Fig. 4d, Extended Data Fig. 9). *daf-2;fkh-9* double mutants were defective in both STAM and learning, and neuronal *fkh-9* expression rescued these defects (Fig. 4e, Extended Data Fig. 9d, e), suggesting that *fkh-9* is required for extended memory and normal neuronal development in *daf-2* mutants. Day 1 and 5 *fkh-9* expression levels correlated with STAM and axon regeneration (Fig. 3d). *fkh-9* reduction delayed development, and reduction during adulthood caused severe matricide (Extended Data Fig. 10a–c). *fkh-9* knockdown in adult *daf-2* worms treated with FUdR (5-fluoro-2′- deoxyuridine) to block matricide[20] significantly shortened lifespan (40–50%; Fig. 4f). Pan-neuronal *fkh-9* expression did not rescue lifespan (Extended Data Fig. 10d), suggesting that FKH-9 acts in non-neuronal tissues to regulate lifespan.

Thus, IIS/FOXO-regulated FKH-9 function is important for both neuronal and non-neuronal growth and development, as well as adult memory and axon regeneration. Interestingly, the FKH-9 mammalian homologue FOXG1 is required for axon outgrowth[23] and is the most highly-induced gene in spinal cords treated with radial glial cell transplant following spinal cord injury[24].

Network analysis using *fkh-9* and the other 8 neuronal DAF-16 STAM genes (Fig. 4g, Supplementary Table 10) identified *casy-1*, which is required for several forms of associative learning and memory[2,25–27], *apl-1*, the *C. elegans* orthologue of amyloid precursor protein (APP) that can disrupt sensory plasticity[28], and *dlk-1*, the only previously known regulator of age-dependent axon regeneration[3,29]. Additionally, genes involved in neuronal degeneration (*mec-17*), neuronal development (*egl-44*, *sem-4*), neuronal function (*egl-21*, *rcn-1*, *vab-9*, *cysl-1*), synaptic regulation and function (*cab-1*, *hlb-1*, *magu-4*, *sph-1*, *unc-64*), and axon outgrowth (*unc-14*) and regeneration (*egl-8*, *fos-1*, *pmk-3*), were connected to the STAM genes. PQM-1 (ref. 8), whose motif (DAE) is overrepresented in neuronal IIS target promoters, and other IIS (*akt-2*, *dct-6*, *hlh-30*), TGF-β (*daf-14*, *sma-4*, *crm-1*, *sma-9*, *sma-1*, *sta-1*), and MAPK pathway (*vhp-1*, *pmk-3*) components emerged in the network. Transcriptional regulation by IIS/FOXO and its targets may lead to broader, indirect transcriptional and non-transcriptional regulation of genes with important neuronal functions.

Plasticity in development, reproduction and longevity allows organisms to respond appropriately to nutrient availability and changes in their environment. The IIS pathway is a critical mediator of these decisions, with FOXO selecting transcriptional targets to execute specific biochemical functions in each tissue, including factors that maintain cognitive function with age. *daf-2* mutant worms maintain neuronal behaviours with age by using a set of transcriptional targets that are distinct from previously identified metabolic and stress resistance targets expressed in other tissues. These genes may regulate additional neuronal targets through non-transcriptional mechanisms (Fig. 4g). The regulation of tissue-specific transcriptional programs is important to coordinate phenotypic responses, extending neuronal abilities in concert with the extended longevity and reproductive span of *daf-2* mutants.

Online Content Methods, along with any additional Extended Data display items and Source Data, are available in the online version of the paper; references unique to these sections appear only in the online paper.

Received 28 May; accepted 25 November 2015.
Published online 14 December 2015.

1. Murphy, C. T. *et al.* Genes that act downstream of DAF-16 to influence the lifespan of *Caenorhabditis elegans*. *Nature* **424,** 277–283 (2003).
2. Kauffman, A. L., Ashraf, J. M., Corces-Zimmerman, M. R., Landis, J. N. & Murphy, C. T. Insulin signaling and dietary restriction differentially influence the decline of learning and memory with age. *PLoS Biol.* **8,** e1000372 (2010).
3. Byrne, A. B. *et al.* Insulin/IGF1 signaling inhibits age-dependent axon regeneration. *Neuron* **81,** 561–573 (2014).
4. Sjöberg, J. & Kanje, M. Insulin-like growth factor (IGF-1) as a stimulator of regeneration in the freeze-injured rat sciatic nerve. *Brain Res.* **485,** 102–108 (1989).
5. Wolkow, C. A., Kimura, K. D., Lee, M. S. & Ruvkun, G. Regulation of *C. elegans* life-span by insulinlike signaling in the nervous system. *Science* **290,** 147–150 (2000).
6. Libina, N., Berman, J. R. & Kenyon, C. Tissue-specific activities of *C. elegans* DAF-16 in the regulation of lifespan. *Cell* **115,** 489–502 (2003).
7. Luo, S., Kleemann, G. A., Ashraf, J. M., Shaw, W. M. & Murphy, C. T. TGF-β and insulin signaling regulate reproductive aging via oocyte and germline quality maintenance. *Cell* **143,** 299–312 (2010).
8. Tepper, R. G. *et al.* PQM-1 complements DAF-16 as a key transcriptional regulator of DAF-2-mediated development and longevity. *Cell* **154,** 676–690 (2013).
9. Zhang, P., Judy, M., Lee, S.-J. & Kenyon, C. Direct and indirect gene regulation by a life-extending FOXO protein in *C. elegans*: roles for GATA factors and lipid gene regulators. *Cell Metab.* **17,** 85–100 (2013).
10. Murakami, H., Bessinger, K., Hellmann, J. & Murakami, S. Aging-dependent and -independent modulation of associative learning behavior by insulin/insulin-like growth factor-1 signal in *Caenorhabditis elegans*. *J. Neurosci.* **25,** 10894–10904 (2005).
11. Tank, E. M. H., Rodgers, K. E. & Kenyon, C. Spontaneous age-related neurite branching in *Caenorhabditis elegans*. *J. Neurosci.* **31,** 9279–9288 (2011).
12. Toth, M. L. *et al.* Neurite sprouting and synapse deterioration in the aging *Caenorhabditis elegans* nervous system. *J. Neurosci.* **32,** 8778–8790 (2012).
13. Chikina, M. D., Huttenhower, C., Murphy, C. T. & Troyanskaya, O. G. Global prediction of tissue-specific gene expression and context-dependent gene networks in *Caenorhabditis elegans*. *PLOS Comput. Biol.* **5,** e1000417 (2009).
14. Ewald, C. Y., Landis, J. N., Abate, J. P., Murphy, C. T. & Blackwell, T. K. Dauer-independent insulin/IGF-1-signalling implicates collagen remodelling in longevity. *Nature* **519,** 97–101 (2015).
15. Zhang, S., Banerjee, D. & Kuhn, J. R. Isolation and culture of larval cells from *C. elegans*. *PLoS ONE* **6,** e19505 (2011).
16. Spencer, W. C. *et al.* Isolation of specific neurons from *C. elegans* larvae for gene expression profiling. *PLoS ONE* **9,** e112102 (2014).
17. Schafer, J. C. *et al.* IFTA-2 is a conserved cilia protein involved in pathways regulating longevity and dauer formation in *Caenorhabditis elegans*. *J. Cell Sci.* **119,** 4088–4100 (2006).
18. Apfeld, J. & Kenyon, C. Regulation of lifespan by sensory perception in *Caenorhabditis elegans*. *Nature* **402,** 804–809 (1999).
19. Hansen, M., Hsu, A.-L., Dillin, A. & Kenyon, C. New genes tied to endocrine, metabolic, and dietary regulation of lifespan from a *Caenorhabditis elegans* genomic RNAi screen. *PLoS Genet.* **1,** 119–128 (2005).
20. Shaw, W. M., Luo, S., Landis, J., Ashraf, J. & Murphy, C. T. The *C. elegans* TGF-β Dauer pathway regulates longevity via insulin signaling. *Curr. Biol.* **17,** 1635–1645 (2007).
21. Lakhina, V. *et al.* Genome-wide functional analysis of CREB/long-term memory-dependent transcription reveals distinct basal and memory gene expression programs. *Neuron* **85,** 330–345 (2015).
22. Chen, L. *et al.* Axon regeneration pathways identified by systematic genetic screening in *C. elegans*. *Neuron* **71,** 1043–1057 (2011).
23. Tian, N. M., Pratt, T. & Price, D. J. Foxg1 regulates retinal axon pathfinding by repressing an ipsilateral program in nasal retina and by causing optic chiasm cells to exert a net axonal growth-promoting activity. *Development* **135,** 4081–4089 (2008).
24. Chang, Y.-W. *et al.* Rapid induction of genes associated with tissue protection and neural development in contused adult spinal cord after radial glial cell transplantation. *J. Neurotrauma* **26,** 979–993 (2009).
25. Ikeda, D. D. *et al.* CASY-1, an ortholog of calsyntenins/alcadeins, is essential for learning in *Caenorhabditis elegans*. *Proc. Natl Acad. Sci. USA* **105,** 5260–5265 (2008).
26. Hoerndli, F. J. *et al.* A conserved function of *C. elegans* CASY-1 calsyntenin in associative learning. *PLoS ONE* **4,** e4880 (2009).
27. Ohno, H. *et al.* Role of synaptic phosphatidylinositol 3-kinase in a behavioral learning response in *C. elegans*. *Science* **345,** 313–317 (2014).
28. Ewald, C. Y. *et al.* Pan-neuronal expression of APL-1, an APP-related protein, disrupts olfactory, gustatory, and touch plasticity in *Caenorhabditis elegans*. *J. Neurosci.* **32,** 10156–10169 (2012).
29. Hammarlund, M., Nix, P., Hauth, L., Jorgensen, E. M. & Bastiani, M. Axon regeneration requires a conserved MAP kinase pathway. *Science* **323,** 802–806 (2009).
30. Wong, A. K., Krishnan, A., Yao, V., Tadych, A. & Troyanskaya, O. G. IMP 2.0: a multi-species functional genomics portal for integration, visualization and prediction of protein functions and networks. *Nucleic Acids Res.* **43,** W128–W133 (2015).

Supplementary Information is available in the online version of the paper.

Acknowledgements We thank the *C. elegans* Genetics Center for strains; WormBase (WS250); L. Parsons for RNA-seq data support; J. Wiggins and the Lewis-Sigler High Throughput Sequencing Core Facility for RNA-seq support; C. DeCoste and the Flow Cytometry Facility for assistance; V. Yao for tissue prediction analysis; R. DiLoreto for chemotaxis assay analysis; and Z. Gitai, the Murphy lab, and W. Mair for discussion. Funding was provided by a Keck Scholars Program fellowship (C.T.M.), National Institutes of Health Cognitive Aging R01 (C.T.M.), Ruth L. Kirschstein National Research Service Awards (R.K., R.A.), National Science Foundation (J.L.) and New Jersey Commission on Brain Injury Research (V.L.) fellowships.

Author Contributions C.T.M., R.K., V.L. and J.L. designed experiments. R.K., V.L., R.A., J.L., J.A., and C.T.M. performed experiments and analysed data. R.K., V.L. and J.L. performed tissue isolation and RNA-seq. A.W., R.K., V.L. and J.L. performed bioinformatics analysis. R.K., V.L. and R.A. performed short-term memory experiments. V.L. performed axon regeneration experiments. R.K., V.L. and C.T.M. wrote the manuscript. R.A. and A.W. contributed equally to this work.

Author Information Sequencing reads are deposited at NCBI BioProject under accession number PRJNA297798. Reprints and permissions information is available at www.nature.com/reprints. The authors declare no competing financial interests. Readers are welcome to comment on the online version of the paper. Correspondence and requests for materials should be addressed to C.T.M. (ctmurphy@princeton.edu).

METHODS

Adult cell isolation. Day 1 adult neuronally GFP-labelled worms (*Punc119::GFP or Pmec-4::GFP*) were prepared for cell isolation as previously described[15] with modifications (Extended Data Fig. 2). Synchronized adult worms were washed with M9 buffer to remove excess bacteria. The pellet (~250 µl) was washed with 500 µl lysis buffer (200 mM DTT, 0.25% SDS, 20 mM HEPES pH 8.0, 3% sucrose) and resuspended in 1,000 µl lysis buffer. Worms were incubated in lysis buffer with gentle rocking for 6.5 min at room temperature. The pellet was washed 6× with M9 and resuspended in 20 mg ml^{-1} pronase from *Streptomyces griseus* (Sigma-Aldrich). Worms were incubated at room temperature (<20 min) with periodic mechanical disruption by pipetting every 2 min. When most worm bodies were dissociated, leaving only small debris and eggs, ice-cold PBS buffer containing 2% fetal bovine serum (Gibco) was added. RNA from FACS-sorted neurons was prepared for RNA-seq and subsequent analysis (see Extended Data for details).

No statistical methods were used to predetermine sample size. The experiments were not randomized, and the investigators were not blinded to allocation during experiments and outcome assessment.

Short-term associative memory assay. Memory assays were performed as described[2].

Axon regeneration assays. *In vivo* laser axotomy of PLM neurons was performed as described[22].

31. Tomioka, M. *et al.* The insulin/PI 3-kinase pathway regulates salt chemotaxis learning in *Caenorhabditis elegans*. *Neuron* **51,** 613–625 (2006).
32. Kodama, E. *et al.* Insulin-like signaling and the neural circuit for integrative behavior in *C. elegans*. *Genes Dev.* **20,** 2955–2960 (2006).
33. Murakami, H., Bessinger, K., Hellmann, J. & Murakami, S. Aging-dependent and -independent modulation of associative learning behavior by insulin/insulin-like growth factor-1 signal in *Caenorhabditis elegans*. *J. Neurosci.* **25,** 10894–10904 (2005).
34. Stein, G. M. & Murphy, C. T. *C. elegans* positive olfactory associative memory is a molecularly conserved behavioral paradigm. *Neurobiol. Learn. Mem.* **115,** 86–94 (2014).

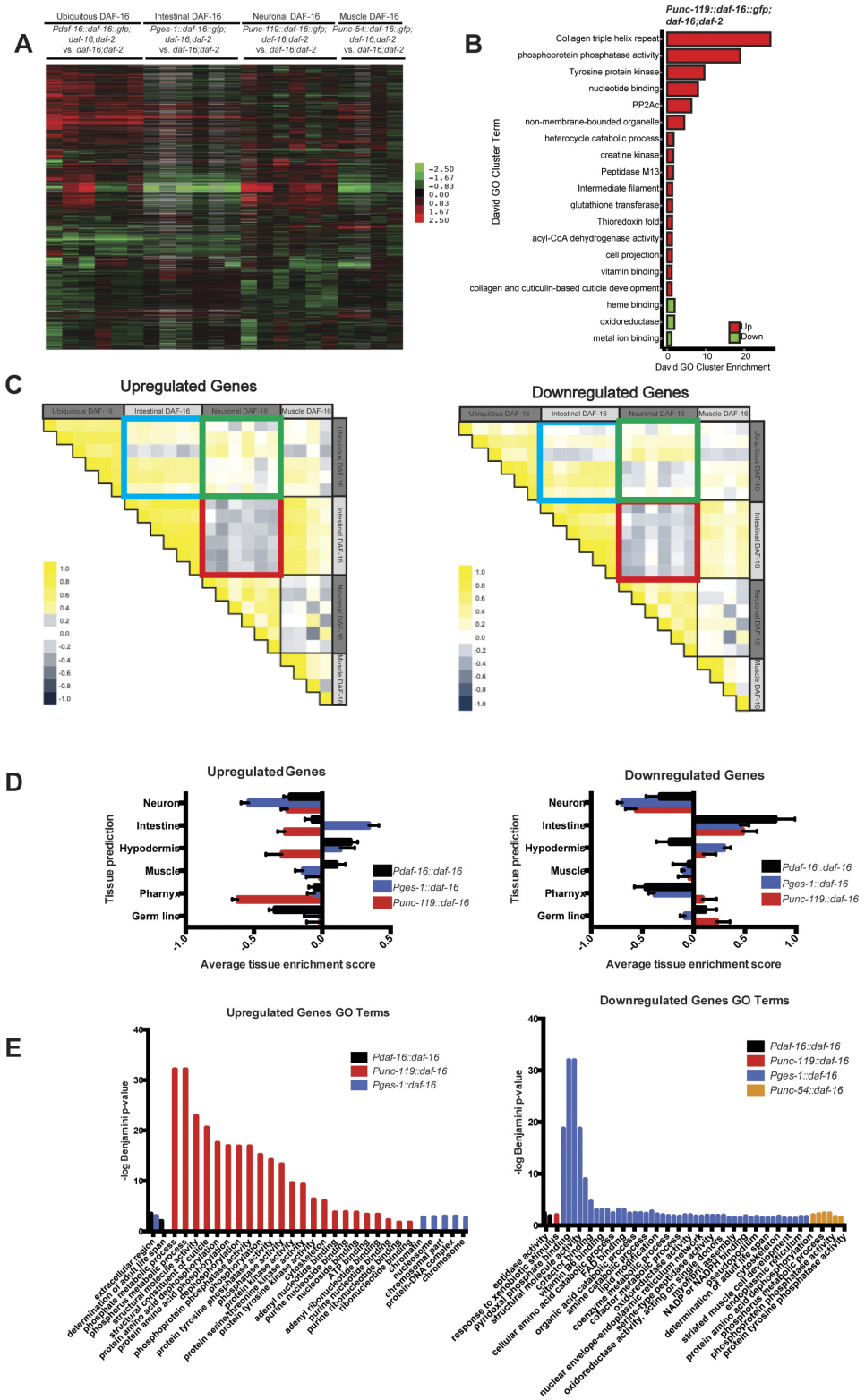

Extended Data Figure 1 | Tissue-specific rescue of DAF-16 activity in *daf-16;daf-2* mutants identifies distinct gene expression profiles. **a**, DAF-16 tissue-specific transgenics; heatmap of all genes with expression differences ≥1.5-fold in ≥3 arrays. **b**, Significant gene ontology (GO) cluster terms from *Punc-119::daf-16*-regulated up- and downregulated genes (enrichment score >1). **c**, Pairwise Pearson correlations between arrays of DAF-16-upregulated or downregulated targets. The red box highlights the negative correlation between neuronal DAF-16 rescued targets (*Punc-119::daf-16::gfp;daf-16;daf-2 vs daf-16;daf-2*) and intestinal DAF-16 targets (*Pges-1::daf-16::gfp;daf-16;daf-2 vs daf-16;daf-2*), while the blue box shows the positive correlation between intestinal DAF-16 targets (*Pges-1::daf-16::gfp;daf-16;daf-2 vs daf-16;daf-2*) and whole-worm DAF-16 targets (*Pdaf-16::daf-16::gfp; daf-16;daf-2 vs daf-16;daf-2*). The green box shows the weak correlation between neuronal rescued and whole-worm DAF-16 targets. **d**, Tissue enrichment analysis (mean ± s.e.m.) of significant DAF-16-rescued up- and downregulated genes (Supplementary Table 1) (FDR <0.5). **e**, Significant GO terms (adjusted *P* value < 0.05) for DAF-16 upregulated and downregulated genes from whole worm, intestine-, neuron- and muscle-rescued DAF-16 strains. Genes used for GO analysis (Supplementary Table 2) were derived from SAM analysis of the microarrays in **a** and Supplementary Table 1.

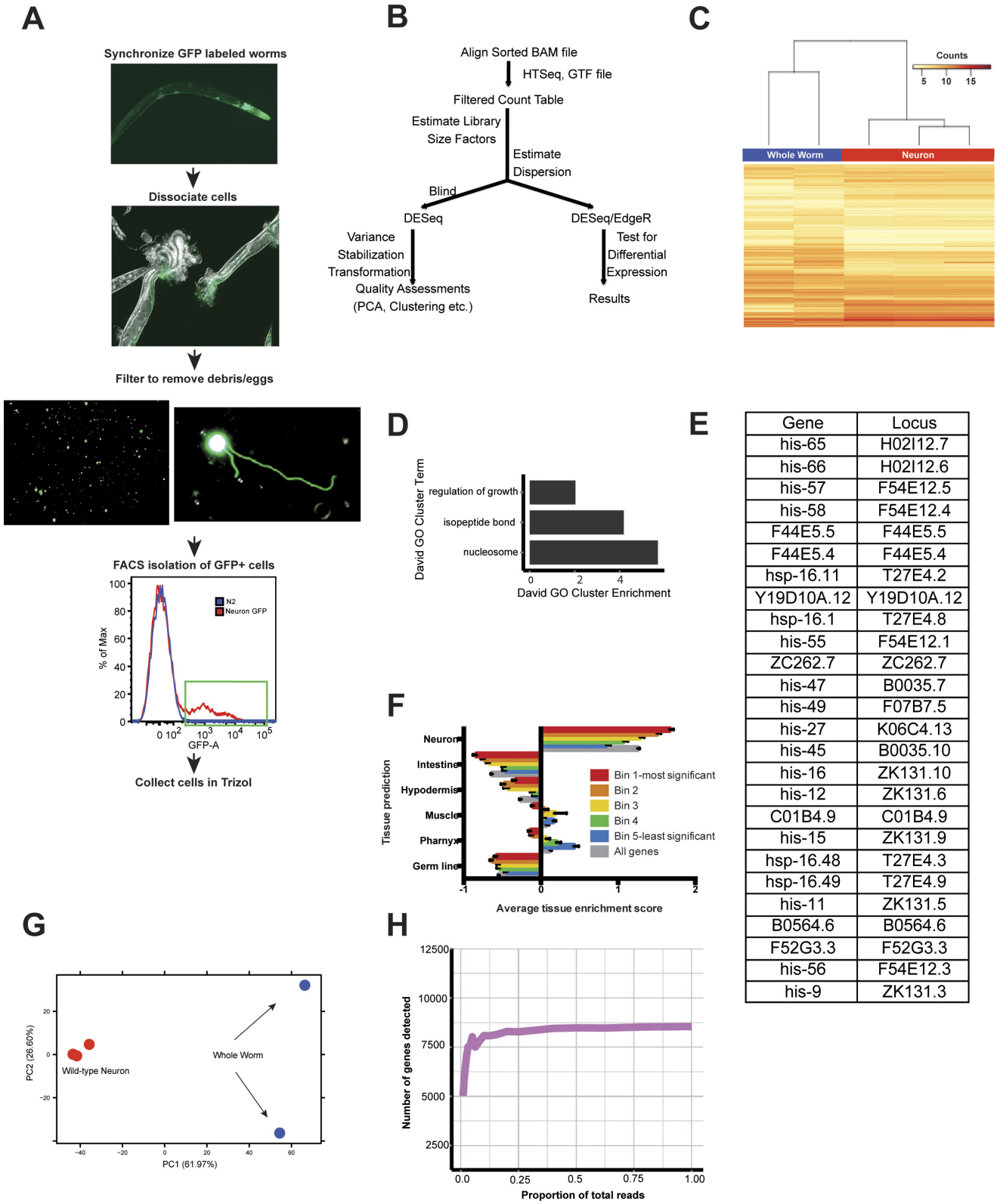

Gene	Locus
his-65	H02I12.7
his-66	H02I12.6
his-57	F54E12.5
his-58	F54E12.4
F44E5.5	F44E5.5
F44E5.4	F44E5.4
hsp-16.11	T27E4.2
Y19D10A.12	Y19D10A.12
hsp-16.1	T27E4.8
his-55	F54E12.1
ZC262.7	ZC262.7
his-47	B0035.7
his-49	F07B7.5
his-27	K06C4.13
his-45	B0035.10
his-16	ZK131.10
his-12	ZK131.6
C01B4.9	C01B4.9
his-15	ZK131.9
hsp-16.48	T27E4.3
hsp-16.49	T27E4.9
his-11	ZK131.5
B0564.6	B0564.6
F52G3.3	F52G3.3
his-56	F54E12.3
his-9	ZK131.3

Extended Data Figure 2 | Protocol for isolating neuron-specific targets using FACS followed by RNA-sequencing. a, Pipeline for isolation of adult cells for FACS and RNA sequencing. **b**, Workflow for RNA-seq data analysis of isolated neurons. **c**, Heatmap of wild-type neuron-expressed relative to whole-worm-expressed genes. **d**, Actinomycin D (transcription inhibitor) treatment (100 μg ml^{-1}) during the cell isolation process demonstrates that the neuron isolation technique induces minimal transcriptional changes in wild type animals. Gene ontology (GO) terms represent genes upregulated in the absence of actinomycin D (Fig. 1b, Supplementary Table 4). **e**, The 26 differentially expressed genes from actinomycin D treatment are listed. **f**, *C. elegans* tissue gene expression prediction confirms neuronal character of adult wild-type neuron-enriched genes. Neuron-enriched genes were divided among equal bins according to *P* value. Bin 1: FDR <0.003%; bin 2: 0.003–0.03%; bin 3: 0.03–1.3%; bin 4: 1.3–4%; bin 5: 4–10%. **g**, Principal component analysis (PCA) shows a clear separation between wild-type adult neuronal and whole-worm samples. **h**, Downsampling of wild-type neuron sequencing reads demonstrates sufficient sampling depth. The number of genes detected at the 3 counts per million threshold (for expressed genes) with different proportions of total sequencing depth analysed.

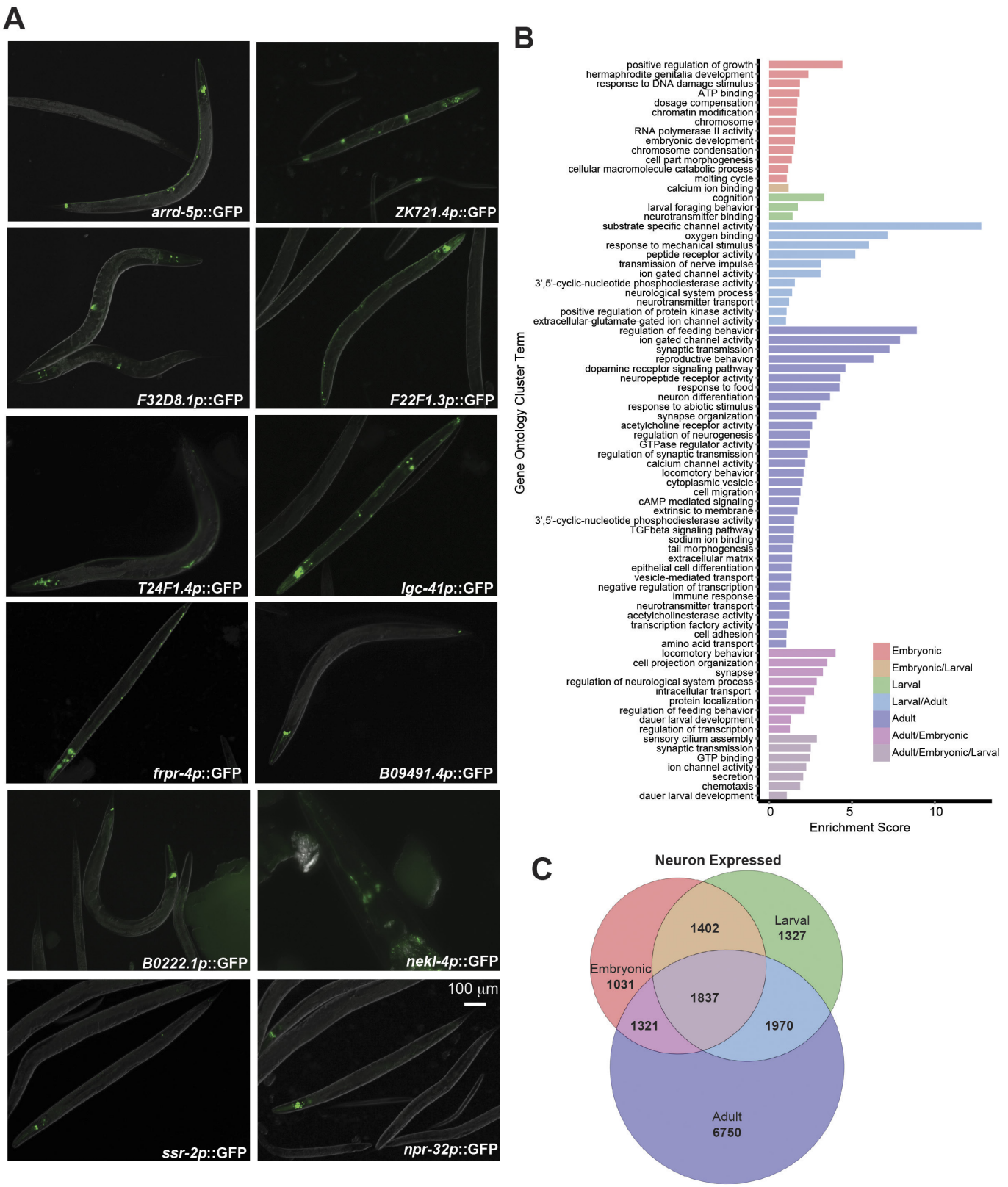

Extended Data Figure 3 | Neuron-expressed genes identified by our method are confirmed to be expressed in adults and have adult neuronal functions. a, Promoter–GFP transcriptional fusions of candidate uncharacterized neuronal genes (day 1 of adulthood). **b**, Gene ontology clusters were generated from the categories in Fig. 1e. Non-overlapping GO terms suggest a transition from development-related processes in embryonic and larval animals to neuronal processes involved in behaviour in adults (Supplementary Table 5). **c**, Venn diagram depicting the overlap between genes classified as "expressed" among embryonic and larval neurons[16] and adult neurons from our RNA-seq analysis (Supplementary Table 5).

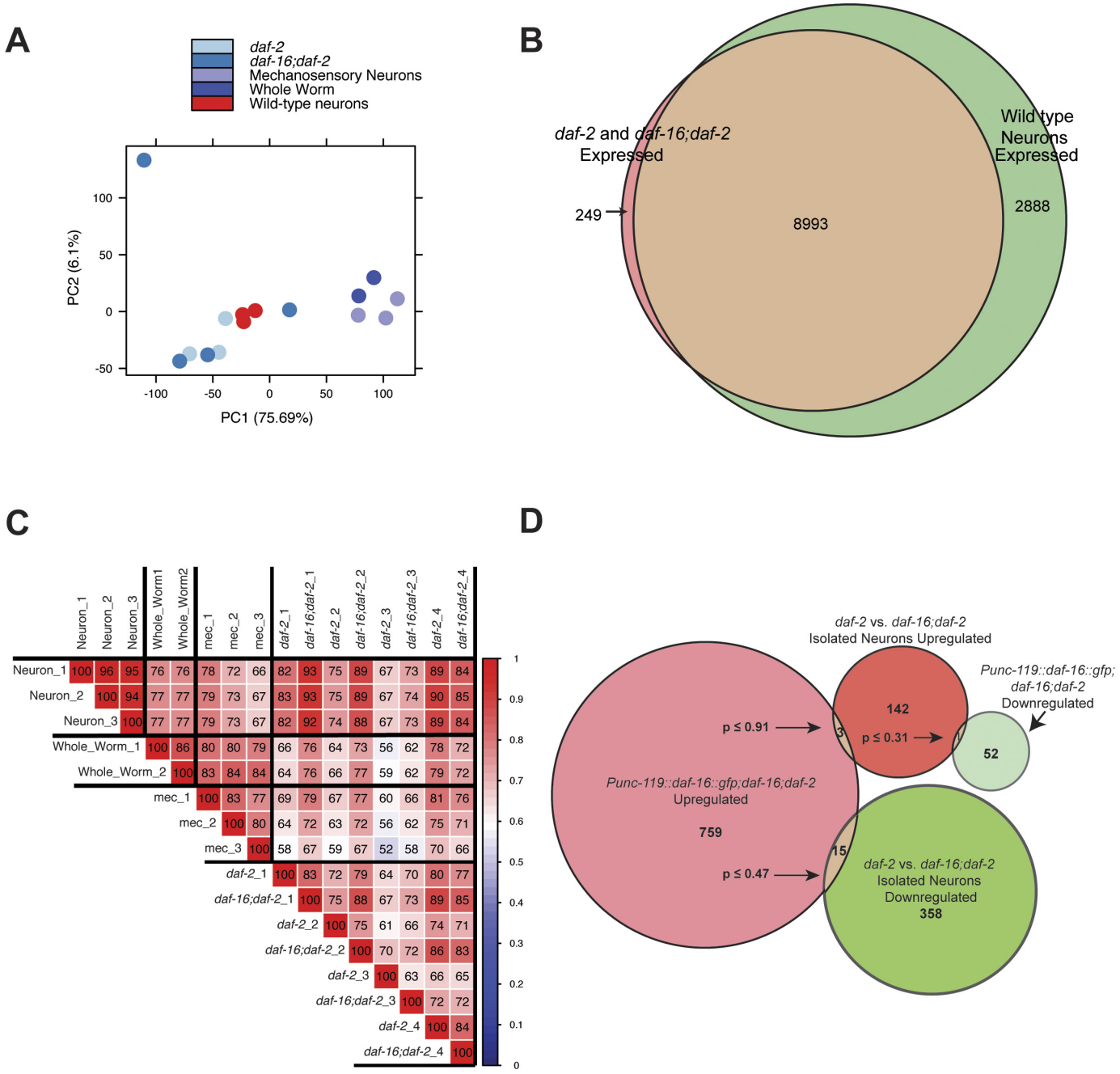

Extended Data Figure 4 | Comparison of neuronal DAF-16 targets with wild-type neuronal targets and whole-worm DAF-16 targets. **a**, Principal component analysis of the whole worm and isolated adult neuron samples obtained for this study. **b**, Venn diagram depicting the overlap of *daf-2*- and *daf-16;daf-2*-expressed genes with those expressed in wild-type adult neurons. **c**, Spearman correlation of whole-worm and isolated adult neuron samples. **d**, The DAF-16 cell-autonomous and cell-non-autonomous targets are distinct. The number of genes that overlap between neuronal DAF-16-rescued whole-worm targets (*Punc-119::daf-16::gfp;daf-16;daf-2 vs daf-16;daf-2*) and isolated neuron IIS targets *(daf-2 vs daf-16;daf-2)* is shown (Supplementary Table 8). Hypergeometric distribution analysis (*P* values) shows that the extent of overlap between the gene categories is not significant.

A

Group	Neuron IIS	Description	% DBE	% DAE
A	Neuron IIS Upregulated	No Overlap with Whole Worm IIS	22.1	21.2
B		Overlap with whole worm IIS upregulated	43.2	21.6
C		Overlap with IIS whole worm downregulated	20	0
D	Neuron IIS Downregulated	No Overlap with Whole Worm IIS	28.2	15.1
E		Overlap with whole worm IIS upregulated	25	18.8
F		Overlap with whole worm IIS downregulated	27.9	27.9

Whole genome occurrence: DBE 30.7%, DAE 20.8%

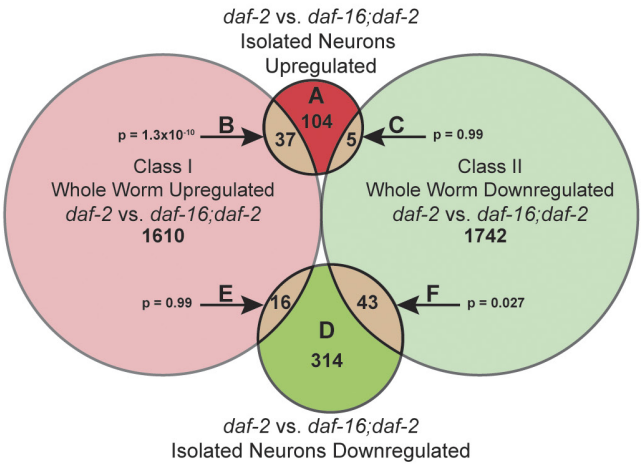

B

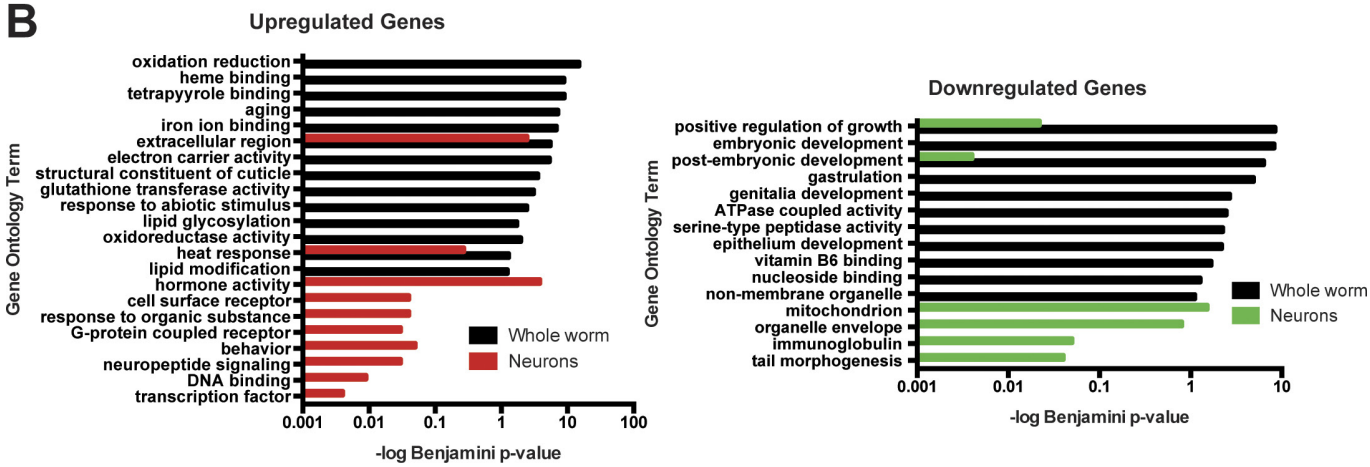

Extended Data Figure 5 | Promoter analysis and gene ontology term analysis of neuronal IIS/FOXO genes. a, The different classes of neuronal IIS/FOXO genes shown in Fig. 2b were analysed for DBE and DAE sequences in the 1 kb upstream promoter regions. The genome-wide percentage of DBE and DAE occurrences across the 1 kb promoters of all gene-encoding regions is reported. Comparison of whole-worm (Class I)[8] vs neuronal-IIS/FOXO-regulated targets. *P* values: hypergeometric distributions. **b**, GO terms of Class I whole worm[8] vs neuronal-IIS upregulated genes (left) and Class II whole worm[8] vs neuronal-IIS downregulated genes (right) (Supplementary Table 5).

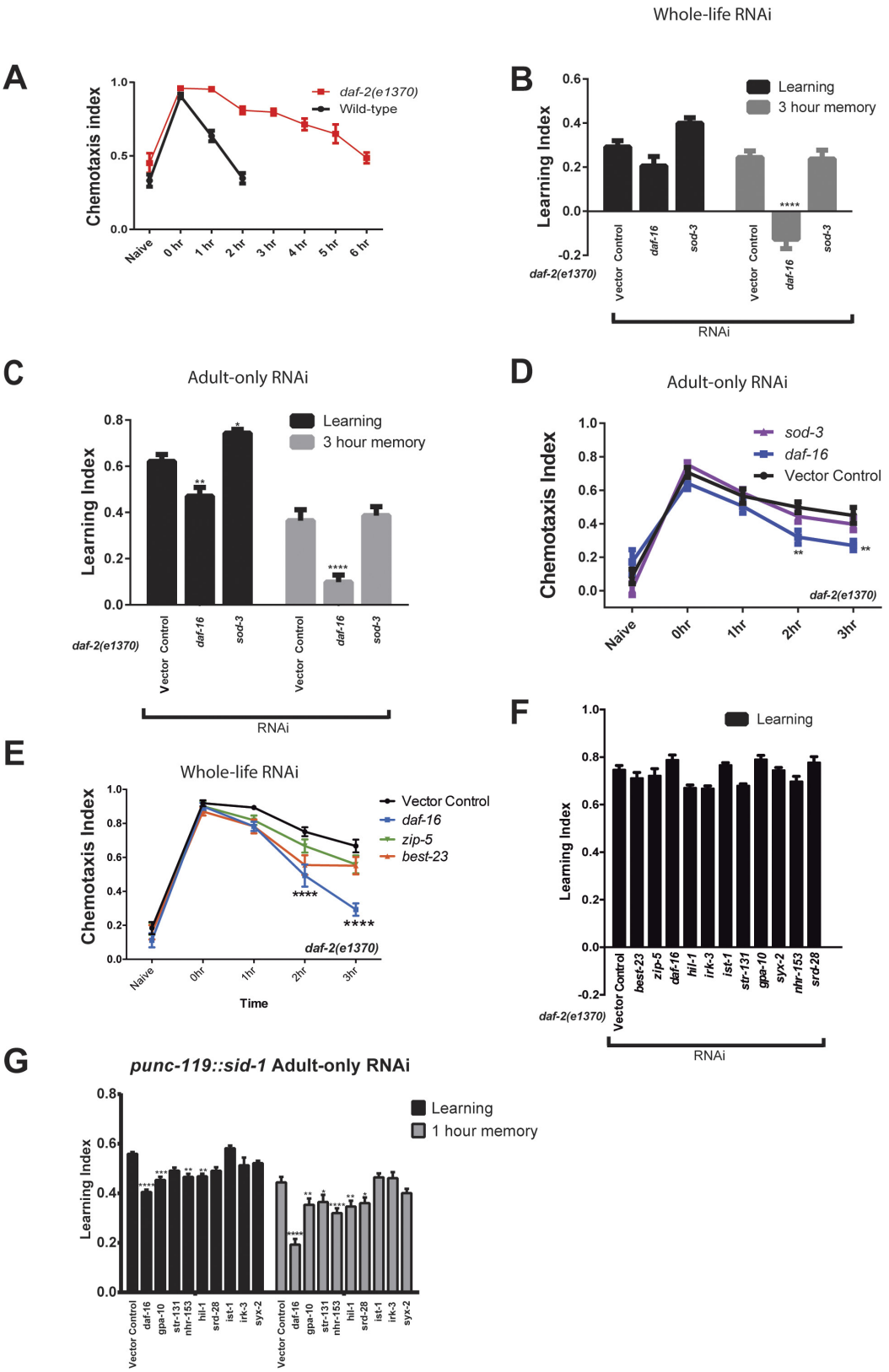

Extended Data Figure 6 | See next page for caption.

Extended Data Figure 6 | Short-term associative memory phenotypes obtained upon knocking down neuronal IIS genes in *daf-2* mutants and wild-type animals. *daf-2* is required for various forms of *C. elegans* associative learning[2,27,31–34]. *daf-16* is required for the improvements and extensions of abilities with age of *daf-2* mutants[2]. *daf-2* mutants are defective for salt chemotaxis learning[27,31,32], and *daf-16* is not involved in salt chemotaxis learning[27,31,32]. Furthermore, salt learning utilizes a unique *daf-2c* isoform[27] in a *daf-16*-independent manner[31], suggesting a learning mechanism distinct from the associative memory paradigms studied here. We are specifically interested in understanding how activation of DAF-16 results in the improved and extended abilities of *daf-2* mutants to carry out olfactory associative learning[2], short-term associative memory[2,34], and long-term associative memory[2], all of which require *daf-16*. **a**, Chemotaxis index profile of wild type (N2) and *daf-2* animals at time points following memory training. **b**, RNAi knockdown of *sod-3*, a non-neuronal DAF-16-regulated target that influences lifespan, has no effect on the extended short-term associative memory (STAM) of *daf-2* mutants when treated with RNAi-feeding bacteria throughout the whole life (**b**) or only the post-developmental (adult-only) period (**c**, **d**) of the animal. *daf-2* worms treated with *daf-16* RNAi have defective STAM, as previously reported[2]. **e**, Knockdown of the neuronal IIS candidate genes *zip-5* and *best-23* does not affect STAM. Time-courses showing the chemotaxis index for each time point are shown in **d** and **e**. Learning indices are shown in **b**, **c**, **f** and **g**. **b**–**e**, Two-way repeated measures ANOVA, Bonferroni post hoc tests. **f**, Treatment of *daf-2* worms with neuronal DAF-16 target RNAi does not affect short-term associative learning. **g**, Neuronal-RNAi sensitive worms (*Punc-119::sid-1*) in a wild-type background were treated only during adulthood with RNAi targeted against the neuronal DAF-16 target genes. Learning (0 h) and 1 h short-term associative memory time points are shown. **a**–**g**, Mean ± s.e.m., $*P < 0.05$, $**P < 0.01$, $***P < 0.001$, $****P < 0.0001$.

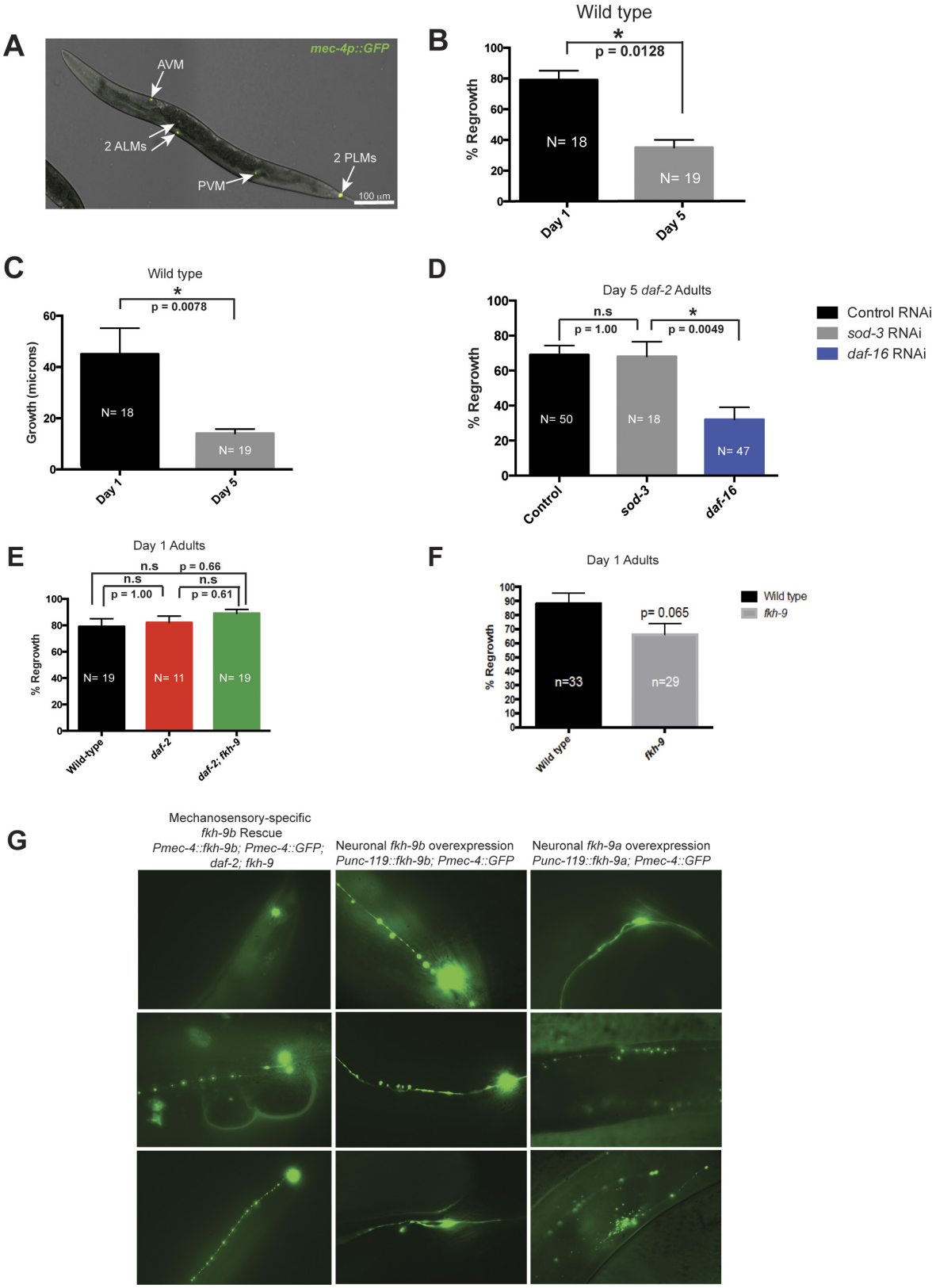

Extended Data Figure 7 | Characterization of age-dependent axon regeneration and structural defects upon *fkh-9* overexpression in mechanosensory neurons. a, Six adult mechanosensory neurons labelled by *mec-4p::GFP* were isolated for RNA-seq. **b**, Axon length from the cell body to the site of injury was measured in µm immediately after axotomy and 24 h later. Regenerative capacity of wild-type PLM axons declines from day 1 to day 5 of adulthood. **c**, Day 5 wild-type animals regrow axons that are significantly shorter than in day 1 animals. **d**, Axotomies of *daf-2* mutants grown on vector control, *sod-3*, or *daf-16* RNAi demonstrate that *sod-3*, a lifespan-regulating DAF-16 target, does not influence the axon regeneration capacity of *daf-2* worms at day 5 of adulthood. **e**, *fkh-9* does not affect the regenerative capacity of *daf-2* axons on day 1 of adulthood. **f**, *fkh-9* is not required for axon regeneration in day 1 adults. **b**–**f**, Mean ± s.e.m., Fisher's exact test, $*P < 0.05$. **g**, Overexpression of the a and b isoforms of *fkh-9* in wild-type animals causes axonal structural defects. Rescuing *fkh-9* activity in the mechanosensory neurons of *daf-2;fkh-9* mutants results in severe beading and degeneration of axons.

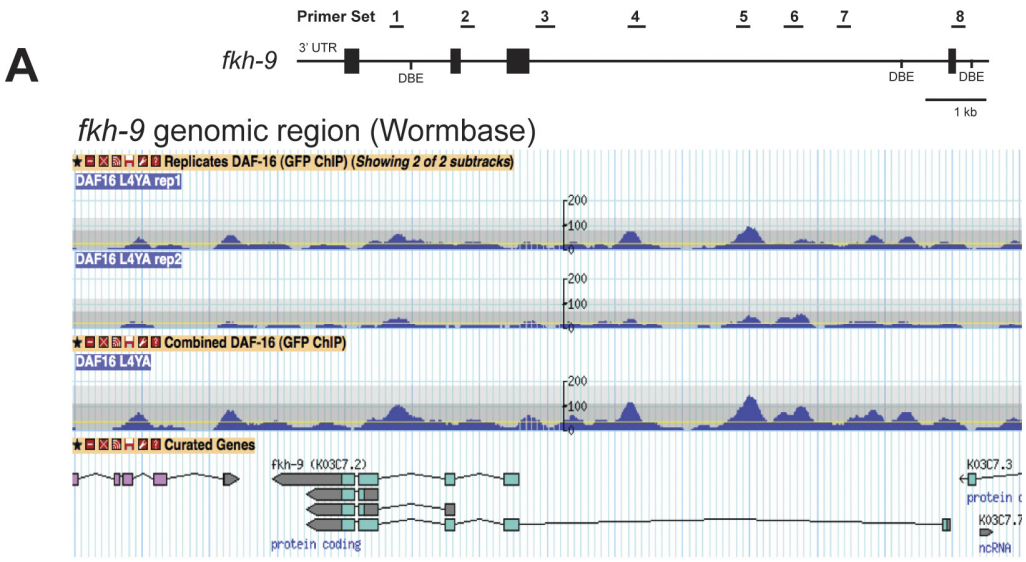

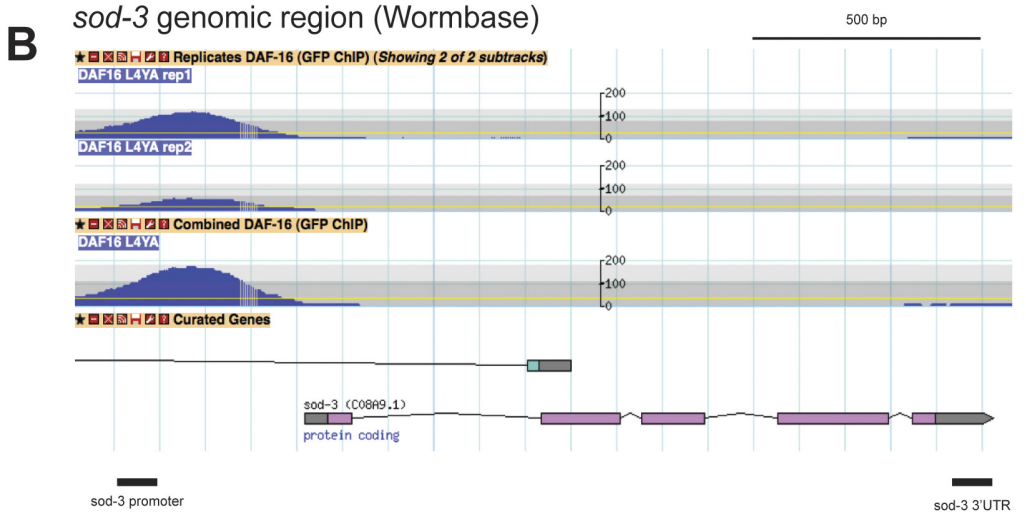

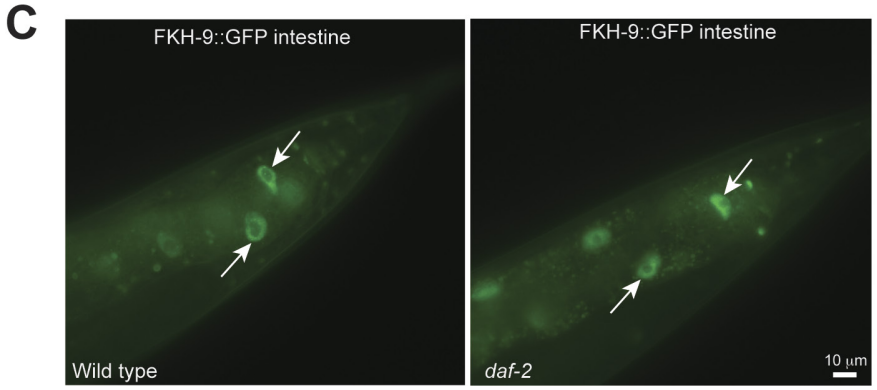

Extended Data Figure 8 | WormBase gene models for *fkh-9* and *sod-3* are shown with modENCODE data for DAF-16 ChIP-seq experiments. **a**, **b**, Wormbase (http://www.wormbase.org) gene models for *fkh-9* (**a**) and *sod-3* (**b**). Primer sets for ChIP-qPCR are depicted in **a**. **c**, Posterior intestinal FKH-9–GFP expression is only modestly increased in *daf-2* compared to wild-type animals expressing *fkh-9p::fkh-9::gfp*. $N = 25$ animals.

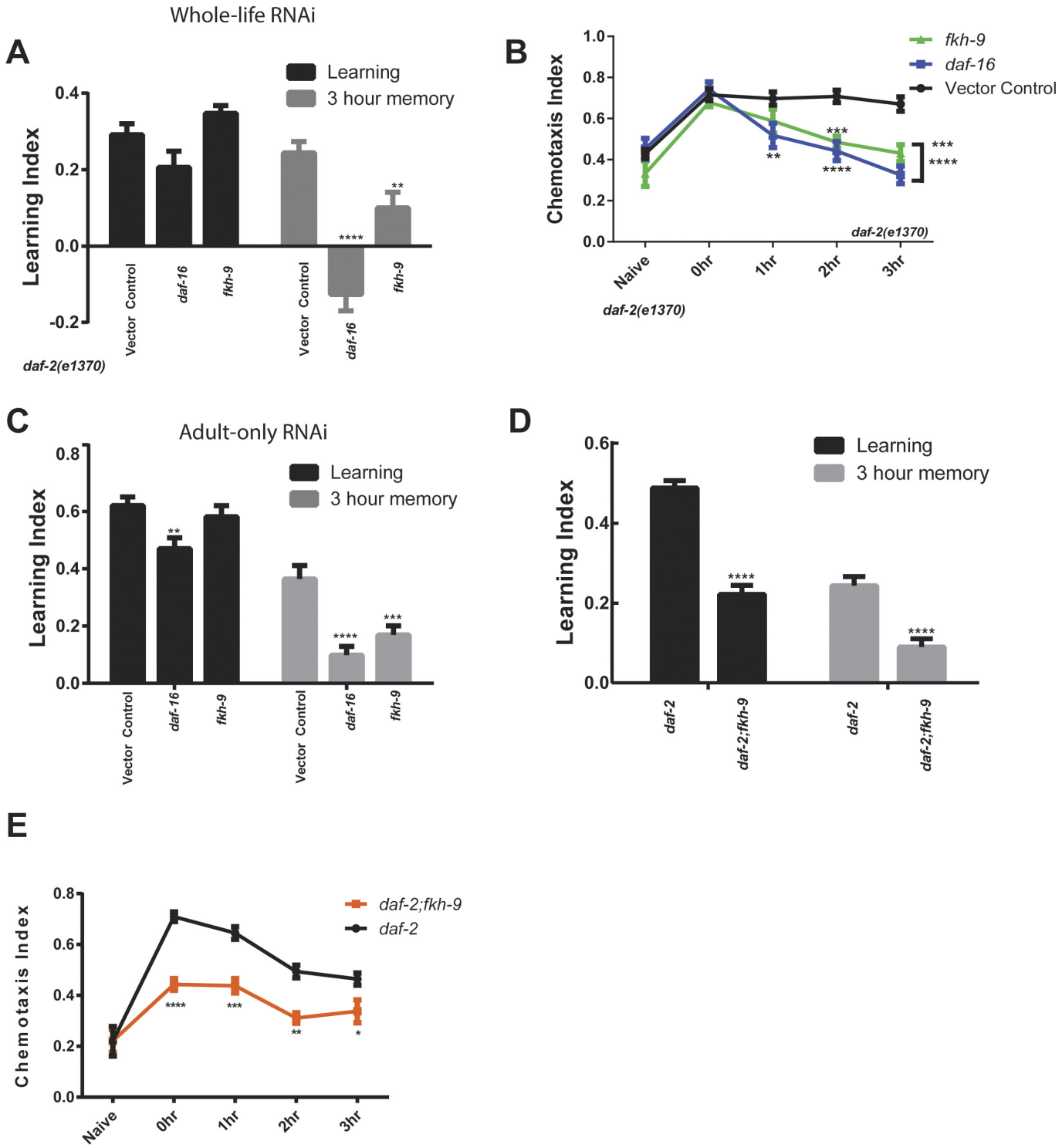

Extended Data Figure 9 | Knocking down *fkh-9* via RNAi or using mutants reduces the enhanced short-term memory of *daf-2* animals. **a**, **b**, Whole-life RNAi of *fkh-9* reduces *daf-2* STAM. **c**, RNAi knockdown of *fkh-9* exclusively during adulthood results in reduced *daf-2* STAM comparable to *daf-16* RNAi-treatment. **d**, **e**, *daf-2;fkh-9* mutants have reduced learning (tested immediately following STAM training) and STAM compared to *daf-2*. Mean ± s.e.m., $*P < 0.05$, $**P < 0.01$, $***P < 0.001$, $****P < 0.0001$. Time-courses showing the chemotaxis index for each time point are shown in **b** and **e**. Learning indices are shown in **a**, **c** and **d**.

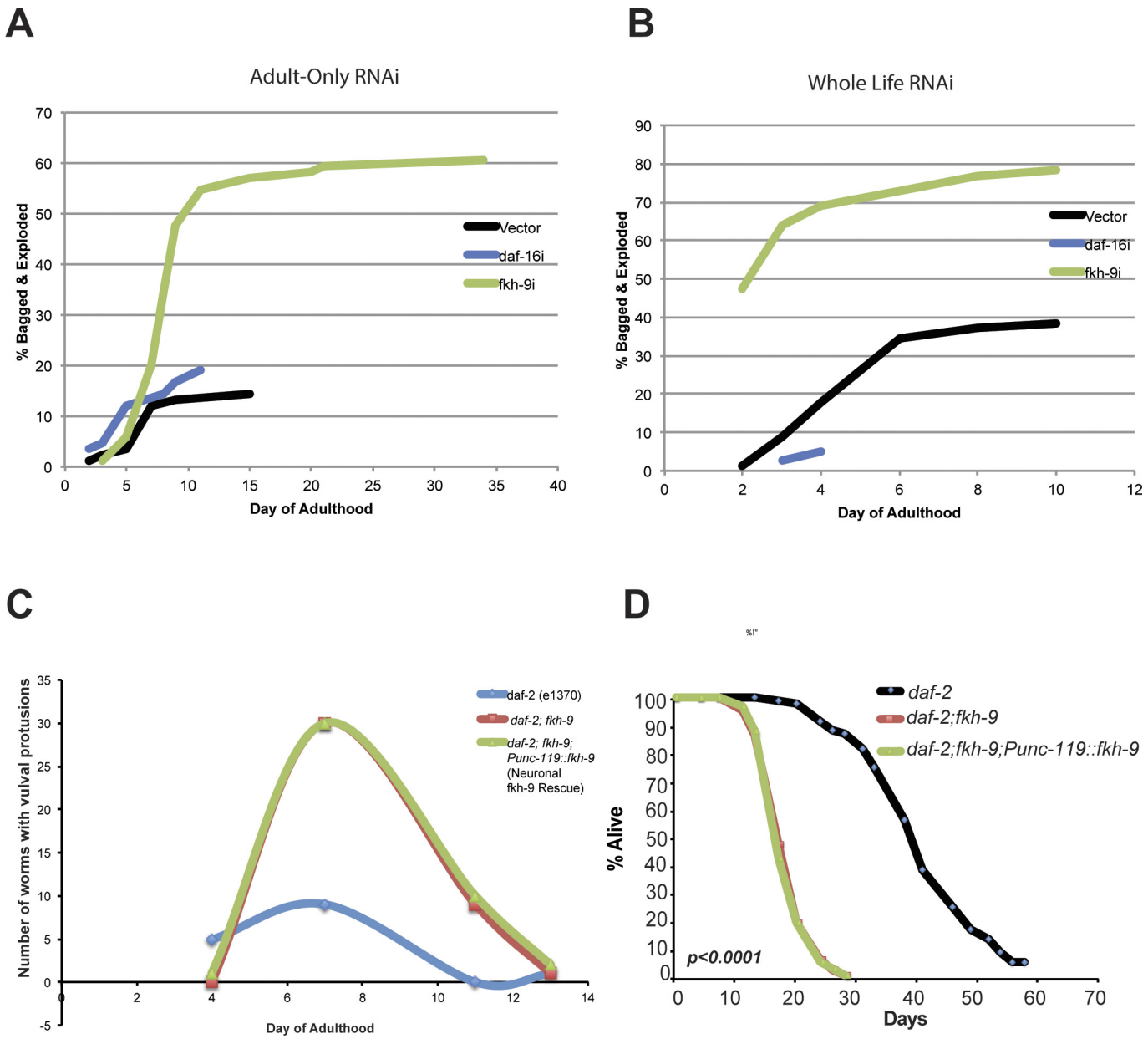

Extended Data Figure 10 | Neuronal FKH-9 is not required for the enhanced lifespan of *daf-2* mutants. a, **b**, Adult-only (**a**) or whole-life (**b**) *fkh-9* RNAi treatment increases matricide in *daf-2* worms. The cumulative percentage of animals dead as a result of bagging and/or exploding was recorded every other day. Two biological replicates were performed, with a representative experiment shown. **c**, Neuronal rescue of *fkh-9* in *daf-2;fkh-9* animals does not diminish the rate of vulval protrusions with age. $N \geq 60$ per conditions for each experiment. **d**, Neuronal rescue of *fkh-9* does not restore longevity of the *daf-2;fkh-9* double mutant. *daf-2* median lifespan: 41 days, *daf-2;fkh-9* 20 days, *daf-2;fkh-9;Punc-119::fkh-9* 20 days. $P < 0.0001$ for *daf-2* vs both *daf-2;fkh-9* and *daf-2;fkh-9; Punc-119::fkh-9*. $N = 112$ worms per strain. Censor rate for *daf-2* 19%, *daf-2;fkh-9* 51%, *daf-2;fkh-9;Punc-119::fkh-9* 56%.